RESEARCH ARTICLE

A multiobjective multi-view cluster ensemble technique: Application in patient subclassification

Sayantan Mitra☯*, **Sriparna Saha**☯

Department of Computer Science and Engineering, Indian Institute of Technology Patna, India

☯ These authors contributed equally to this work.
* sayantaniem@gmail.com

Citation: Mitra S, Saha S (2019) A multiobjective multi-view cluster ensemble technique: Application in patient subclassification. PLoS ONE 14(5): e0216904. https://doi.org/10.1371/journal.pone.0216904

Editor: Yang Li, Northeast Electric Power University, CHINA

Received: February 17, 2019

Accepted: April 30, 2019

Published: May 23, 2019

Data Availability Statement: Underlying data owned by Ron Shamir's Lab at Tel Aviv University, Israel, are available here: http://acgt.cs.tau.ac.il/multi_omic_benchmark/download.htm. Further underlying datasets may be found at the following: https://www.ncbi.nlm.nih.gov/geo/query/acc.cgi?acc=GSE22219 for OXF.BRC.1 and OXF.BRC.1 datasets for GSE22219 https://www.ncbi.nlm.nih.gov/geo/query/acc.cgi?acc=GSE22220 for OXF.BRC.1 and OXF.BRC.1 datasets for GSE22220 http://cbio.mskcc.org/cancergenomics/prostate/data/ for MSKCC.PRCA.

Abstract

Recent high throughput omics technology has been used to assemble large biomedical omics datasets. Clustering of single omics data has proven invaluable in biomedical research. For the task of patient sub-classification, all the available omics data should be utilized combinedly rather than treating them individually. Clustering of multi-omics datasets has the potential to reveal deep insights. Here, we propose a late integration based multiobjective multi-view clustering algorithm which uses a special perturbation operator. Initially, a large number of diverse clustering solutions (called base partitionings) are generated for each omic dataset using four clustering algorithms, viz., k means, complete linkage, spectral and fast search clustering. These base partitionings of multi-omic datasets are suitably combined using a special perturbation operator. The perturbation operator uses an ensemble technique to generate new solutions from the base partitionings. The optimal combination of multiple partitioning solutions across different views is determined after optimizing the objective functions, namely *conn*-XB, for checking the quality of partitionings for different views, and agreement index, for checking agreement between the views. The search capability of a multiobjective simulated annealing approach, namely AMOSA is used for this purpose. Lastly, the non-dominated solutions of the different views are combined based on similarity to generate a single set of non-dominated solutions. The proposed algorithm is evaluated on 13 multi-view cancer datasets. An elaborated comparative study with several baseline methods and five state-of-the-art models is performed to show the effectiveness of the algorithm.

Introduction

In the field of biology and medicine, classification has wide range of applications [1]. With the advancement in microarray technology, generation of thousands of gene sequence data points for cancer-tissue datasets has become possible. It is possible to accurately differentiate between different categories of cancers by analyzing the gene expression values of cancer tissues over different conditions or time points. Classification of patients into subgroups can improve the

Funding: Dr. Sriparna Saha gratefully acknowledges the Young Faculty Research Fellowship (YFRF) Award, supported by Visvesvaraya PhD scheme for Electronics and IT, Ministry of Electronics and Information Technology (MeitY), Government of India, being implemented by Digital India Corporation (formerly Media Lab Asia) for carrying out this research. The funders had no role in study design, data collection and analysis, decision to publish, or preparation of the manuscript.

Competing interests: The authors have declared that no competing interests exist.

diagnostic and treatment. Available methods for patient stratification are dependent on gene sequence data and patients are grouped based on the expression profiles [2, 3]. In addition to gene sequence data other data types, like miRNA (microRNA) expression, DNA methylation, can be explored to improve the accuracy of patient classification models [4]. Each of these data is termed 'omic' (genomics, transcriptomics, methylomics, respectively). The objective here is to identify groups with similar molecular characteristics.

Integrative clustering of several omics data for the same set of samples can disclose more precise structures that are not exposed by examining a single omic data. By exploiting the information present in multiple omics, clustering techniques can obtain better performance compared to a single omic. Some of the advantages of clustering based on multiple omics are given as follows: (i) multi-omics clustering reduces the effect of noise in the data, (ii) each omic can reveal structures that are not present in other omics, (iii) different omics can unfold different cellular aspects.

A major difficulty of cluster analysis is the selection of best clustering algorithm for a given data set [5].Many omic datasets possess heterogeneous structures whereas most of the existing clustering algorithms search for homogeneous structures from a dataset. The problem of algorithm selection for clustering datasets having heterogeneous structures can be addressed by combined use of cluster ensemble and multi-objective clustering techniques [6].

Recently, Li et al. [7] proposed a novel method of combining multi-objective optimization (MOO) with integrated decision making (IDM) to address the problem of combined heat and power economic emission dispatch. Authors used a two-stage approach. In the first stage, θ–dominance based evolutionary algorithm is used to generate Pareto-optimal front of the model. In the second stage, using fuzzy c-means clustering, the obtained Pareto-optimal solutions are clustered to identify the best compromise solutions using grey relation projection.

In this paper, the clustering problem is formulated as an optimization problem where different cluster quality measures are used as the objective functions. We have introduced a multi-objective based multi-view cluster ensemble algorithm (*enAMOSA*, in short), which simultaneously uses the concepts from both cluster ensemble and multi-objective based multi-view clustering algorithms. The key idea is to minimize problems associated with cluster analysis, as well as to overcome the limitations of multi-objective based multi-view clustering and cluster ensemble methods when they are used separately. Here ensemble is not used as a late-integration technique, but it is used as a perturbation operator for generating new solutions based on the selected parent solutions. Throughout this paper, omic is termed as view and multi-omic as multi-view in the context of algorithms. An overview of the proposed method is given below:

- *enAMOSA* conducts multi-view based multi-objective clustering by first identifying different partitions from the same data set using different views. To capture the goodness of an individual clustering generated using a single view, an internal cluster validity index, *conn*-XB index [8], is used. The values of the *conn*-XB index for different partitions obtained using varying views are simultaneously optimized along with agreement index [9]. Agreement index measures the agreement among multiple partitions obtained using different views in a new way. A special perturbation operator is used which replaces the traditional mutation operator. This operator uses an ensemble method along with the initial population for generating new diverse solutions. Finally, the partitions obtained on multiple views are combined to generate a single solution.
- A large number of experiments are conducted to illustrate the efficacy of different components of the proposed *enAMOSA* algorithm. We have developed several baseline methods by generating all possible combinations of the base partitions used in the experiment. These

baselines are explained in detail in the later sections of the paper. To further demonstrate the effectiveness of the proposed perturbation operator, we have also compared results of *enAMOSA* with another version of multi-view AMOSA where normal perturbation operator is used (the perturbation operator used in [9]) and ensemble technique is used separately for combining the final Pareto optimal solutions generated by different clustering algorithms.

- The developed algorithm is tested on 13 genomic datasets. Results are compared with those obtained by baseline algorithms and existing state-of-the art models.

The overall steps of the proposed algorithm are shown in Fig 1.

Some of the contributions of our proposed methodology are as follows:

- To the best of our knowledge, this work is the first multi-objective based multi-view approach for capturing heterogeneous structures from multi-omics data in the field of patient classification.
- A new perturbation operator is designed by combining the concepts of both multi-objective multi-view clustering and cluster ensemble. It improves the robustness of the proposed algorithm to deal with data having different types of clusters.
- The algorithm is capable of capturing heterogeneous structures within a view and also amongst different views.
- In our proposed algorithm, different views can be clustered using different clustering algorithms. Further, the views can have a different number of clusters. To the best of our knowledge, previous multi-view multi-objective algorithms, like MvAMOSA [9], allow different

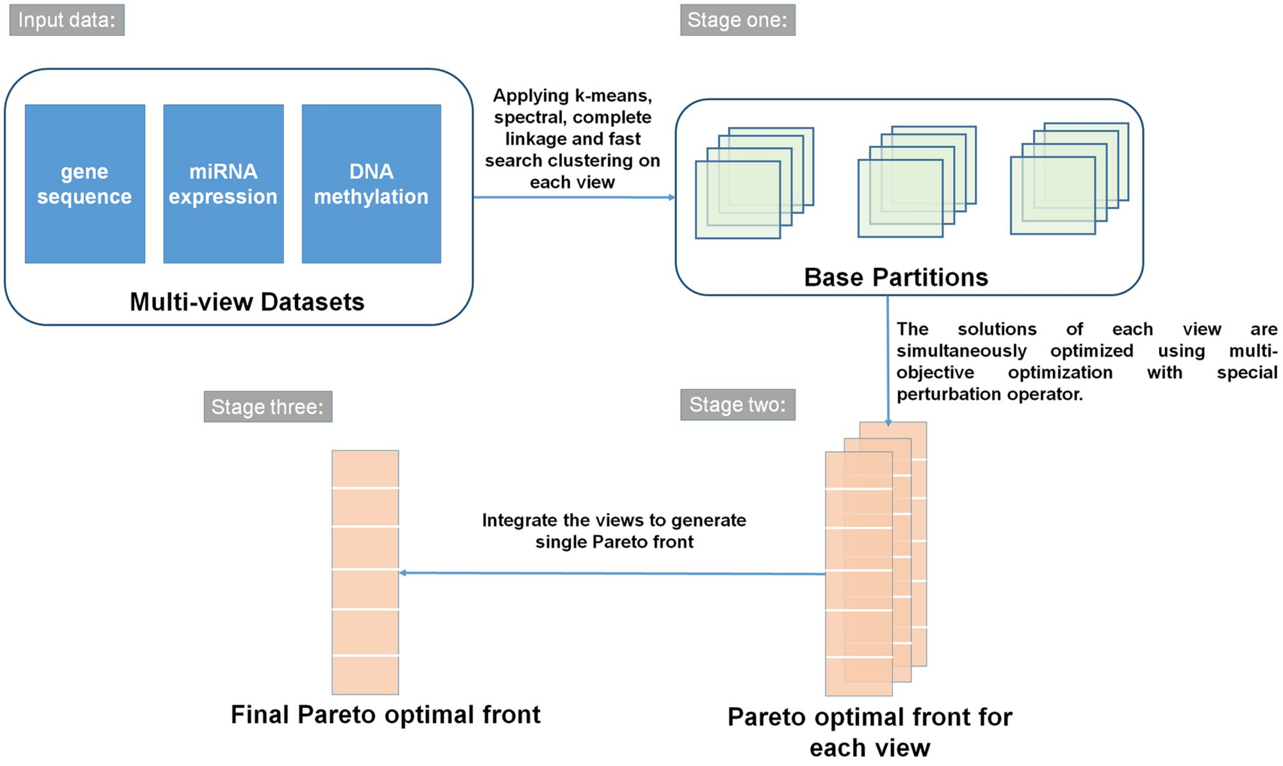
Input data:
gene sequence
miRNA expression
DNA methylation
Multi-view Datasets
Applying k-means, spectral, complete linkage and fast search clustering on each view
Stage one:
Base Partitions
The solutions of each view are simultaneously optimized using multi-objective optimization with special perturbation operator.
Stage two:
Stage three:
Integrate the views to generate single Pareto front
Final Pareto optimal front
Pareto optimal front for each view

Fig 1. Overview of the proposed algorithm *enAMOSA*.

https://doi.org/10.1371/journal.pone.0216904.g001

views to be clustered by the same clustering algorithm and also restrict all the views to have the same number of clusters.

Background

In the literature, several semi-supervised or supervised classification methods [10–12] are developed for cancer diagnosis. These classification techniques classify tumor samples in cancer dataset as malignant or benign or any other sub types [13]. But it is not always possible to obtain labeled tissue samples. For example, real life gene expression datasets in Ref. [14] or microRNA datasets in Ref. [15] are some unlabeled datasets. Hence, application of supervised classification techniques in cancer classification problem is difficult due to unavailability of labeled data. Thus clustering techniques become popular in solving different problems from bioinformatics domain. Multiple molecular profiling data can be collected for the same individual. Exploiting these data separately and then combining them can significantly improve the clinically relevant patient subclassifications [16].

This section discusses existing works on multi-view clustering, cluster ensemble techniques, drawbacks of the state-of-the art models and motivation of the work.

Existing works on multi-omics/view clustering methods

The increase of multi-modal datasets in real-world applications has raised the interest in multi-view learning [17].

Based on the algorithmic approach multi-view clustering methods can be broadly classified into three categories; (i) Early integration, (ii) Late integration, and (iii) Intermediate integration.

Early integration approach is the simplest amongst all. In this approach, at first, all the different views are concatenated to form a single large dataset with features from multiple views. The resulted dataset is clustered using any single-view clustering method. However, this approach has some major drawbacks. Firstly, it causes a significant increase in the data dimension which is a challenge for clustering algorithms. Secondly, it ignores different distributions present in different views of the dataset. LRACluster [18] and Structured sparsity [19] are some of the methods which use early integration approach. LRACluster [18], uses a latent representation of the samples to determine the distribution of numeric, count and binary features. It optimizes a convex objective and provides a globally optimal solution. Structured sparsity [19] method concatenates the views and applies a weighted linear transformation for clustering. The features that do not contribute to the cluster structure are assigned with low weights.

In late integration approach, each view of the dataset is clustered separately using a single-view algorithm. Here, each view can be clustered using different clustering algorithms. Finally, the clusters from different views are integrated to form combined global clusters. COCA [20] and PINS [21] are examples of methods using this approach. PINS [21] uses a connectivity matrix to integrate clusters of different views. This algorithm first adds some Gaussian noise to the data, the cluster number is chosen in a way that clustering is robust to the perturbation. Serra et al. [16], proposed a multi-view approach, MVDA, for identifying different clinically relevant patient-subclasses by combining the information present in multiple high-throughput molecular profiling data sets generated by omics technologies.

Intermediate integration approach involves the following; (i) methods where views are integrated using similarity/distance, (ii) methods that use joint dimension reduction for different views and (iii) methods using statistical modelling of the views.

Chikhi [22], proposed a generalized spectral clustering algorithm, Multi-View Normalized Cuts (MVNC). It is a two-step approach. Initially, the spectral clustering is applied on the dataset followed by a local search to refine the initial clustering. Similarity Network Fusion (SNF) [23] is another similarity-based method which constructs a similarity network for each view separately. Using an iterative process these networks are fused together. Regularized Multiple Kernel Learning with Locality Preserving Projections (rMKL-LPP) [24], performs dimensionality reduction on different views such that similarities amongst the samples are preserved in low dimensions. Subsequently, K-means is applied to this low dimensional representation. Zhang et al. in [25], proposed CMVNMF (Constrained Multi-View clustering based on NMF). It is an extension of the NMF model where different views can contain different samples, but certain samples from different views are constrained to be in the same cluster. iCluster [26] utilized a joint latent-variable model to detect the grouping structure from multi-omics data. iCluster+ [27], an extension of iCluster, includes different models but maintains the idea of iCluster that data originates from a low dimension. The latest extension is iClusterBayes [28]. This method uses Bayesian regularization and is much faster compared to its previous variants. In [29], authors proposed an parameter-free clustering models, Adaptively Weighted Procrustes technique, for multiview clustering. Authors in [30], proposed a self weighted multiview clustering technique (SwMC).

Existing works on cluster ensemble

Cluster ensemble is a technique of deriving a better clustering solution from a set of candidate clustering solutions [5, 31]. A cluster ensemble algorithm can be presented as a two step approach: (i) a diverse set of base partitions are generated; and (ii) these partitions are combined to form a single consensus partition. Depending on the type of base partitions, cluster ensemble is of two types, viz., homogeneous and heterogeneous. When base partitions are obtained from same clustering algorithm, it is called homogeneous and in contrast if base partitions are obtained from different clustering algorithms, it is called heterogeneous. Based on the type of consensus function used, the existing approaches of cluster ensemble are mainly categorized under co-association, graph/hyper-graph partitioning, mutual information or re-labeling [6].

In [32], authors formalized the cluster ensemble problem as a combinatorial optimization problem in terms of shared mutual information. They have proposed three algorithms: MCLA (meta- clustering algorithm), cluster-based similarity partitioning algorithm (CSPA) and hyper-graph partitioning algorithm (HGPA). Depending on the mutual information shared, a consensus function can be applied to select the best partition amongst those produced by these three algorithms.

Based on the base partitions, the CSPA algorithm constructs a similarity matrix. Values in the matrix denote the fraction of partitions where two objects belong to the same cluster. Further, a similarity-based clustering algorithm is applied on this matrix to generate the consensus partitioning.

In HGPA algorithm, a hypergraph is constructed by representing base partition clusters as hyper-edges of the graph. This hypergraph is partitioned by cutting with a minimal number of hyper-edges.

In MCLA algorithm, a meta-graph is constructed, where each base partition cluster forms the vertex. Similarity between the vertices represents the edge weights of this graph. Vertices belonging to the same partition do not have edges. On partitioning the meta-graph, the clusters belonging to the same group are considered correspondents. The objects are assigned to the meta-clusters they are strongly associated with, generating the consensus partition.

In the HBGF (Hybrid bipartite graph formulation) HBGF [33], a bipartite graph is constructed from the set of base partitions. Objects and clusters are simultaneously modeled as vertices of the graph. In the end, a graph partitioning algorithm is applied on the generated bipartite graph. The resulting division of the objects is the consensus partitioning.

Drawbacks of the existing literature

In the field of patient sub-classification, multi-view data from multiple omics technologies can be obtained for same individual. The clinically relevant patients sub-classification can be significantly improved by combining these data, rather than exploiting them separately. However, by and large, multi-view clustering approaches have not penetrated bioinformatics yet [34]. The existing multi-view based classification techniques for patient sub-classification suffer from the following drawbacks:

1. Existing multi-view clustering problems are mostly solved as single objective optimization problems. A single quality measure for partitioning is optimized implicitly or explicitly using various paradigms of unsupervised single-view learning. Initially different views of the dataset are partitioned and later the agreement between the partitions obtained on different views is optimized. But instead of treating these two objectives (goodness of partitions obtained using individual views and agreement among-st partitions) separately, it is better to optimize them simultaneously for capturing better partitioning structures among the views.
2. The existing multi-view based approaches applied for patient sub-classification problem are very simple in structure and cannot effectively identify more than one relevant structures of the datasets.
3. Multi-objective clustering algorithms can identify different alternative partitionings of a dataset after a single execution. But as the number of alternatives increases, the analysis becomes harder.
4. In the patient-stratification problem, cluster ensemble is mostly used during view integration. But, the literature lacks the use of any multi-view multi-objective algorithm combinedly with an ensemble technique rather than separately, to capture fine-structures present among different views.
5. Most of the existing multi-view algorithms are designed to capture homogeneous structures among multiple views.
6. Existing multi-view multi-objective algorithms allow the same clustering algorithm for partitioning the data over multiple views of the sample and also restrict the views to have the same number of clusters.

Motivation

The general aim of any multi-view clustering is to improve the cluster quality in each view and to increase the agreement between multiple partitionings obtained using individual views. By nature it is a multi-objective optimization problem with two types of objectives, cluster quality over different views and agreement between multiple views, to be optimized simultaneously. Further, multi-omics datasets exhibit complex structures, difficult for single-objective based clustering algorithms to capture. Although the multi-objective approach offers a set of alternative structures of the dataset, as the number of alternatives increases, the analysis becomes harder. All these motivated us to develop a new multi-objective based multi-view algorithm with a unique ensemble based perturbation operator that is capable of capturing the fine-tuned structures in multi-omic datasets.

Problem formulation

The multi-view cluster ensemble problem is formulated as a multiobjective optimization problem.

- Given:
  - A multi-view dataset containing V views and n number of samples $S = \{\bar{x}_1, \bar{x}_2, \ldots, \bar{x}_n\}$,
  - d_m is the number of features in the m^{th} view, and D^m is the $n \times d_m$ matrix representing the m^{th} view.
  - D^m_{ij} is the j^{th} feature of the i^{th} sample in the m^{th} view.
  - Concatenation of the V views produces matrix D of size $n \times d$, where $d = \sum_{m=1}^{V} d_m$ is the total number of features.
  - A set of base clustering algorithms, $CA_1, CA_2, \ldots, CA_p$.
  - A set of objective functions

    $$CV_1, CV_2, \ldots, CV_m, AI,$$

    where each CV_i is a cluster validity index measured on the partitioning obtained after considering only view m for the given data set, and AI is used for measuring the agreement between the partitions obtained for different views.
- Find:
  - A consensus partitioning (U) generated by ensembling the outputs of clustering algorithms, $CA_1, CA_2, \ldots, CA_p$, satisfying all views
  - The set of samples, S, is divided into K clusters, $\{U_1, U_2, \ldots, U_K\}$
    - $U_i = \{\bar{x}^i_1, \bar{x}^i_2, \ldots, \bar{x}^i_{n_i}\}$; n_i: number of samples in cluster i; $\bar{x}^i_j$: jth sample of cluster i.
    - $\cup_{i=1}^{K} U_i = S$ and $U_i \cap U_j = \emptyset$ for all $i \neq j$.
  - which simultaneously optimizes the objective functions. The simultaneous optimization of these objectives produces a Pareto optimal front.

Materials and methods

enAMOSA: Ensemble based multi-view archived multi-objective simulated annealing

This section discusses about the proposed multiobjective based multi-view cluster ensemble approach, namely *enAMOSA*.

To overcome the difficulties of traditional clustering algorithms, *enAMOSA* combines characteristics of cluster ensemble and multi-view based multi objective clustering methods. *enAMOSA* comprises of three main steps: (1) generation of diverse set of base partitions for each view, (2) determination of an ensembled partitioning considering the multiple base partitions and (3) finally generating a consensus partitioning satisfying different views. The proposed algorithm differs from traditional ensemble approach in two ways. Firstly, instead of producing a single consensus partitioning, it produces a set of consensus partitionings. In fact, the set of solutions can contain partitionings that are combinations of other partitionings, or partitionings of high quality that already appeared in the set of individual partitionings. Secondly, it is an iterative process. For each iteration, it combines pairs of partitionings for each view and then the views are integrated to generate a new solution for evaluation. The steps involved in *enAMOSA* are shown in Algorithm 1.

The calculation of dominance among the solutions is the same as in AMOSA [35]. In the Algorithm 1, temperature (*temp*) plays a significant role in calculating the probability of acceptance of a solution.

Algorithm 1: Algorithm for enAMOSA

```
Initialize: $iter$, $SL$, $HL$, $T_{min}$, $T_{max}$, $no\_views$, $\alpha$, $temp = T_{max}$
begin
  Initialize pool with solutions from k-means, complete linkage,
    fast search clustering and spectral clustering.
  for i = 1 to pool_size do
    for j = 1 to no_views do
      ComputeFitnessconnXB(pool[i], j /* Compute conn-XB for each
        view */
    end
    ComputeFitnessAI(pool[i])
  end
  Compute dominance of the solutions in pool.
  Initialize Archive with the non-dominated solutions of pool
  current = random(Archive)
  while $temp \geq T_{min}$ do
    for gen = 1 to iter do
      new_pt = perturb current
      for j = 1 to no_views do
        ComputeFitnessAI(new_pt[j], j)
      end
      ComputeFitnessAI(new_pt)
      Compute dominance of current and new_pt
      Update Archive and current
    end
    $temp = \alpha \times temp$
  end
  Pareto_front = CombineViews(Archive)
end
```

Generation of base partitions. To generate the initial solutions (called base partitions), four different clustering techniques (called base clustering algorithms), hierarchical (complete linkage) [36], K-means, fast search [37] and Spectral clustering, are applied on each view of the given dataset. These four algorithms used belong to different categories of the clustering algorithm, like, K-means represents the centroid models, hierarchical represents the connectivity model and, spectral and fast search represent the density based model of clustering. The more diverse the base algorithms, higher the chances of capturing differently shaped clusters of the data set. It is essential to have different types of partitionings in the initial archive so that *enAMOSA* can receive as much information as possible to find an optimal number of possible existing structures.

The choice of clustering algorithms for generating base partitions are not merely restricted to these four clustering algorithms only, but other clustering algorithms can also be used.

The number of clusters (K) which will be given as an input to the base clustering algorithm ($\wedge$) is determined randomly. The number of clusters is varied over the range K_{min} to K_{max}. Here, the value of K_{min} = 2 and $K_{max} = \sqrt{n}$, where n denotes the number of samples. A value K is selected randomly between the range K_{min} and K_{max} with uniform probability. $\wedge$ is applied to the data set with the number of clusters = K varying the views.

But fast search [37] is a density-based clustering and parameters are determined automatically from the corresponding views. This algorithm does not consider the number of clusters as input. It automatically determines the number of clusters from any given dataset.

At the end of this step, we have a set of base partitions for each view.

Archive initialization. For each view, we compute the dominance of the base partitions obtained in previous step. A set of non-dominated solutions are generated from each view. The archive is initialized with these non-dominated solutions.

The initial population of the archive in *enAMOSA* is not generated randomly, as is done for most of the AMOSA based clustering techniques. Instead, it is composed of a set of base partitions, π_1, generated by running a diverse set of conceptually different algorithms.

String representation. In order to represent the initial partitioning solutions generated by different clustering algorithms, membership matrix based representation scheme is used.

For example, if K-means is executed on V different views with the corresponding set of attributes with the number of clusters = K, then for each case, a membership matrix, *Mem* of size $K \times n$ is obtained as follows:

$$Mem_{ij} = \begin{cases} 1 & \text{if } \bar{x}_j \in U_i \\ 0 & \text{otherwise} \end{cases}$$

Here, $\bar{x}_j$ denotes the j^{th} data point and U_i denotes cluster i. Mem_{ij} denotes the membership value of the j^{th} data point for the i^{th} cluster.

Suppose the data set is having total V views and the clustering algorithm $\wedge$ is selected to be executed on the data set. Then for a given view, a membership matrix of size $K \times n$ is generated. Total V such membership matrices of size $K \times n$ are encoded in the string. Thus length of the string is $V \times K \times n$. Fig 2 shows an example of the proposed string representation. All the strings of the archive are initialized in the above way.

Perturbation operator. The special perturbation operator uses ensemble method along with initial population for generating new solutions.

This operator finds the consensus partitioning between a pair of selected parents, for each individual view. Any existing cluster ensemble method can be used in *enAMOSA* as the perturbation operator. The idea is to generate new good-quality solutions which are combinations of previous two solutions. First, two parents are randomly selected from the archive to be combined. The combination is done for individual views. Ensemble based operator is applied on the membership matrices present in two selected solutions for a given view. Let π_1^1 and π_1^2, be the membership matrices of two selected solutions, respectively, with K_1^1 and K_1^2 number of clusters (π_1^2 means second selected parent from view 1 and similarly for others). Let the ensembled solutions be represented by π_1^F and π_2^F. The number of clusters K_1^F for partition π_1^F is chosen randomly in the interval $[K_1^1, K_1^2]$. Second, the parents are combined using ensemble method. The consensus partition generated has K_1^F clusters. Illustration of the operator is given in Fig 3. The operator is briefly described in Algorithm 2.

Here, CSPA (cluster-based similarity partitioning algorithm) technique [32] is used as underlying ensemble method. The operator worked as follows:

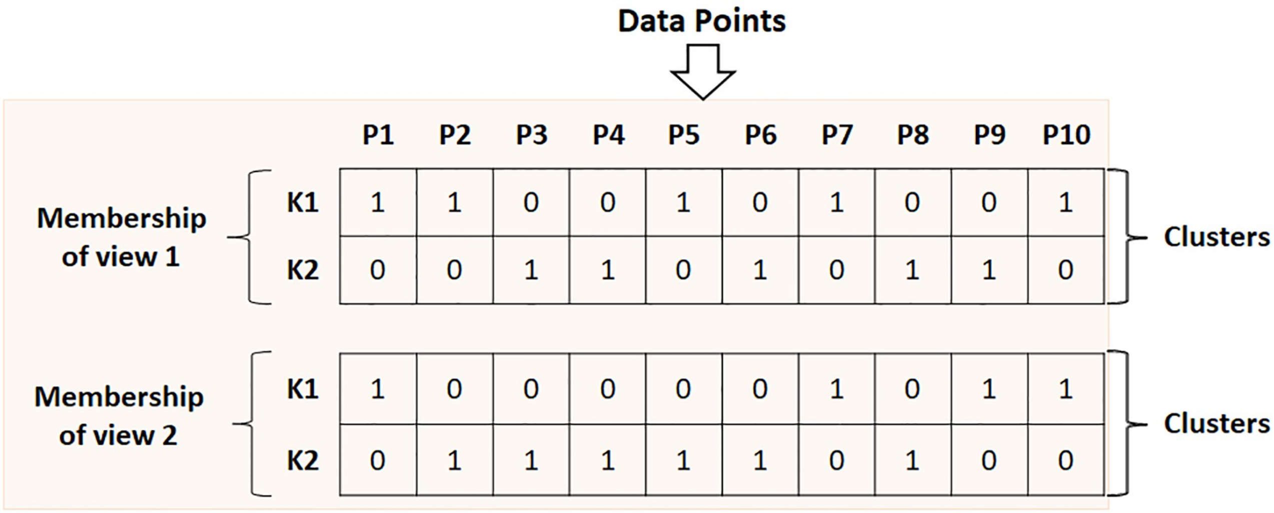

Data Points

		P1	P2	P3	P4	P5	P6	P7	P8	P9	P10	
Membership of view 1	K1	1	1	0	0	1	0	1	0	0	1	Clusters
	K2	0	0	1	1	0	1	0	1	1	0	
Membership of view 2	K1	1	0	0	0	0	0	1	0	1	1	Clusters
	K2	0	1	1	1	1	1	0	1	0	0	

Fig 2. Membership matrices represented in a solution. In the example, there are two views, two clusters, and a data set of ten points.

https://doi.org/10.1371/journal.pone.0216904.g002

- Let the selected clustering solutions be: π^1 and π^2 with K^1 and K^2 number of clusters, respectively. Let the corresponding partitionings be $U_1^1, U_2^1, U_3^1, \ldots, U_{K^1}^1$ and $U_1^2, U_2^2, U_3^2, \ldots, U_{K^2}^1$ corresponding to the solutions, π^1 and π^2, respectively.
- For each partitioning solution, an adjoint matrix, $A_{n\times n}^k$, $k = 1, 2$ is generated as follows:

$$A_{ij}^k = \begin{cases} 1 & \text{if points } i \text{ and } j \text{ belong to the same cluster} \\ 0 & \text{otherwise} \end{cases} \tag{1}$$

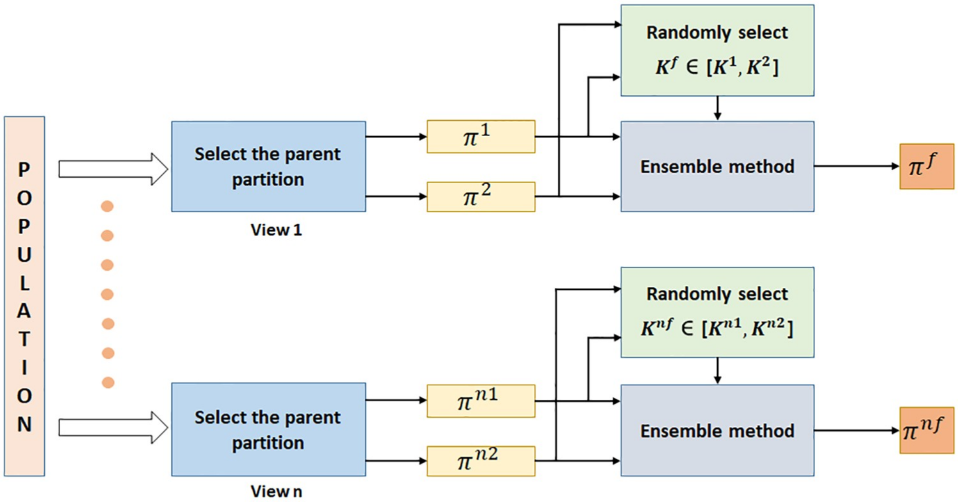
P O P U L A T I O N
Select the parent partition
View 1
π^1
π^2
Randomly select $K^f \in [K^1, K^2]$
Ensemble method
π^f
Select the parent partition
View n
π^{n1}
π^{n2}
Randomly select $K^{nf} \in [K^{n1}, K^{n2}]$
Ensemble method
π^{nf}

Fig 3. *enAMOSA* perturbation operator.

https://doi.org/10.1371/journal.pone.0216904.g003

- A new similarity matrix, $Sim_{n\times n}$ is computed as follows:

$$Sim_{ij} = sum_{k=1}^{2} A_{ij}^{k} \tag{2}$$

This similarity matrix is used for clustering the data set using any standard similarity-based clustering algorithm like hierarchical clustering technique. In general an induced similarity graph (vertex = object, edge weight = similarity) approach using METIS [38] can be used along with the newly generated similarity matrix.

The above ensemble based operator is applied for individual views separately.

Algorithm 2: Algorithm for new perturbation operator.

```
procedure: perturb(Element)
begin
  $Element_2$ = random($Archive$) /*Select a random solution from $Archive$
  except $Element$*/
  for $i$ = 1 to $no\_views$ do
    $K_1$ = no_of_clusters($Element[i]$)
    $K_2$ = no_of_clusters($Element_2[i]$)
    $K_F$ = randi($K_1$, $K_2$) /*Generate integers in range $K_1$ and $K_2$*/
    $new\_pt[i]$ = CSPA($Element[i]$, $Element_2[i]$, $k_F$)
  end
  return $new\_pt$
end
```

Objective functions. The optimization framework uses two objective functions: (i) Agreement Index [9] for measuring the agreement between partitions obtained from different views, and (ii) Connectivity based XB-Index or *conn*-XB Index [8].

Agreement index. Agreement Index [9] is used for measuring the agreement between partitions obtained from different views.

$$AI_{v1,v2} = \frac{n_a + 1}{n_d + 1}, n_a = \sum_{i=1}^{n}\sum_{j=1}^{n} I_{A_{ij}^{v1}, A_{ij}^{v2}}$$

$$n_d = n^2 - n_a$$

$$I_{A_{ij}^{v1}, A_{ij}^{v2}} = \begin{cases} 1 & \text{if } A_{ij}^{v1} = A_{ij}^{v2} \\ 0 & \text{otherwise} \end{cases}$$

Here A^{v1} and A^{v2} are adjoint matrices of the views $v1$ and $v2$ respectively. The final *Agreement index* for the total partitioning is calculated as follows:

$$AI_{total} = \frac{\sum_{l=1}^{V}\sum_{m=1, l\neq m}^{V} 2 \times AI_{v_l, v_m}}{V \times (V - 1)}$$

Here, n total samples in the dataset and V is the number of views.

***connected*-XB or *conn*-XB Index.** In [8], authors have developed connectivity based XB-Index. The definition of this index follows the formulation of popular XB-Index [39].

$$conn - XB = \frac{\sum_{i=1}^{K}(\sum_{\bar{x}\in U_i} d_{short}(\bar{x}, \bar{z}_i))}{n(min_{i,k=1\ldots K, i\neq k} d_{short}(\bar{z}_k, \bar{z}_i))} \tag{3}$$

$d_{short}(\bar{x}, \bar{z}_i)$ is the shortest distance between two points, $\bar{x}$ and $\bar{z}_i$, along the relative neighborhood graph [8]. It measures the connectivity between two points. If two points are connected /

a path exists between these two points along the relative neighborhood graph (RNG) then d_{short} value will be low. Here U_i denotes the cluster i, $\bar{z}_i$ is the medoid of cluster i, n is the size of the whole data set and $\bar{z}_j$ denotes the cluster j. The objective is to lower the value of *conn-XB* index in order to obtain good partitioning.

A solution encodes total V number of membership matrices/partitionings. For each such membership matrix/partitioning, the value of *conn-XB* is calculated to measure the goodness of this partitioning. Let the values be $conn–XB_1$, $conn–XB_2$, . . ., $conn–XB_V$. Then the objective functions corresponding to a single solution are

$$\{conn - XB_1, conn - XB_2, \ldots, conn - XB_V, \frac{1}{AI}\}$$

enAMOSA simultaneously optimizes these $(V + 1)$ number of objective functions.

Algorithm 3: Algorithm for combining views

```
procedure: CombineViews(Archive)
begin
  for i = 1 to archive size do
    Initialize each element of temp_sum with 0 /*Size of temp_sum is
      sample × sample */
    for j = 1 to no_views do
      adj = GenerateAdjMatrix(Archive[i][j]) /*Generate adjacency
        matrix for each view*/
      temp_sum = temp_sum + adj
    end
    Initialize each element of new_adj with 0 /*Size of new_adj is
      sample × sample */
    for k = 1 to sample do
       for l = 1 to sample do
         if $temp\_sum[k][l] > \frac{no\_views}{2}$ then
           new_adj[k][l] = 1
         end
       end
     end
      Generate clusters from new_adj matrix.
   end
end
```

Consensus function for view combination. At the end of the execution of *enAMOSA*, we get a set of non-dominated solutions on the final archive. The psedu code is given in Algoriyhm 1. Each of these solutions encodes total V number of membership matrices. A new late integration method is proposed to combine the membership matrices present in a single solution. A consensus partitioning is obtained satisfying all the available views. So, in order to get a consensus partitioning, initially the common points of different clusters present in different partitionings obtained using different views are identified. This is achieved by majority voting scheme. If a pair of points cluster together in majority of the views then in the final partitioning they will also be grouped together. Likewise all the pairs of data points are evaluated. If some points are not assigned to any group (this situation may occur if even number of views are used and a tie occurs) then in the final partitioning, these points are assigned to the group of their nearest neighbors. The process is illustrated below:

- Let the adjoint marices of the partitionings present in a string corresponding to different views be denoted by A^k where $k = 1 . . . V$, $V = totalnumberofviews$. Then a new adjoint matrix,

A^{sum} is computed as follows:

$$A^{sum}_{ij} = \sum_{k=1}^{V} A_{ij} \tag{4}$$

- Now a new matrix A^{new} is generated as follows:

$$A^{new}_{ij} = \begin{cases} 1 & \text{if } A^{sum}_{ij} > \left\lceil \frac{V}{2} \right\rceil \\ 0 & \text{Otherwise} \end{cases}$$

- The matrix A^{new} is used to generate the final partitioning. Following a link based approach, connected components of the matrix A^{new} are identified. Points are considered as vertices and the points, (i, j), whose $A^{new}_{ij} = 1$ are connected by an edge. The connected components of this graph are treated as initial clusters. Let total number of clusters be K.
- For rest of the points which are not part of any of the clusters extracted in the previous step, cluster assignment is done as follows. Any point $\bar{x}_i$ will be assigned to kth cluster where:

$$k = \operatorname*{argmin}_{k=1}^{K} \min_{j=1}^{n_k} d_{short}(\bar{x}_i, \bar{x}^k_j) \tag{5}$$

  Here K denotes total number of clusters/connected components identified from the previous step. n_k denotes the number of points in the kth connected component/cluster, $\bar{x}^k_j$ denotes jth point of the kth cluster and $d_{short}(\bar{x}_i, \bar{x}^k_j)$ denotes the shortest distance [8] between $\bar{x}_i$ and $\bar{x}^k_j$.
- Finally a partitioning will be obtained where all the points are part of some clusters. This partitioning is reported as the final consensus partitioning for that particular solution.
- For each solution present in the archive, a single consensus partitioning is obtained. If *archive–size* = N, then N such consensus partitionings will be generated.

Theoretical analysis

Complexity analysis. In this section, the time complexity of *enAMOSA* is discussed. The basic steps and their complexities are as follows:

1. Initialization of Archive: $O(SL)$
2. Domination status between two solutions: $O(M)$, where M = number of objectives
3. Domination status between a single solution and archive elements: $O(M \times SL)$
4. Complexity of perturbation (here we used CSPA): $O(n^2 \times r \times \text{TotalIter})$, where n = no. of samples, r = no. of clusters
5. Single linkage clustering: $O(SL^2 \times \log(SL))$
6. Clustering is done:
   - during initialization if $NDom > SL$, where $NDom$ = number of non-dominated solutions.

- after each $|SL{-}HL|$ number of iterations
- if $Archive{-}size > HL$ in the end
  Clustering is executed for $\frac{TotalIter}{(SL-HL)} + 2$ times.

$$\text{Clustering complexity} = O(\frac{TotalIter}{(SL-HL)} \times SL^2 \times \log(SL))$$

Final time complexity of *enAMOSA* is

$$TotalIter \times (SL + M + M \times SL + n^2 \times r + \frac{1}{(SL-HL)} \times SL^2 \times \log(SL))$$

Let $HL = N$, where N = size of Archive and $SL = \gamma \times HL$, $\gamma \geq 2$

$$TotalIter \times (\gamma \times N + M + M \times \gamma \times N + n^2 \times r + \frac{\gamma^2}{(\gamma-1)} \times N \times \log(\gamma \times N))$$

The final time complexity of *enAMOSA* is:

$$O(TotalIter \times (n^2 \times r + N \times (M + \log(N)))) \tag{6}$$

Convergence analysis. In the proposed algorithm *enAMOSA*, we have simultaneously optimized two objectives, *conn*-XB Index [8] and Agreement index [9].

conn-XB Index [8] follows the formulation of popular XB-Index [39]. It measures the ratio between the cluster compactness and cluster separation. Xie-Beni validation index behaves convex when the samples are around the optimal values for the centroids [40]. Similarly, *conn*-XB Index [8] behaves convex under same condition.

Agreement index [9] measures the agreement between partitions obtained using different views. It is given by the following equation:

$$AI = \frac{n_a + 1}{n_d + 1} \tag{7}$$

where, n_a = number of pairs of samples occurring together in both the views.

n_d = number of pairs of samples not occurring together in different views.

If there are n number of samples then,

$$n_d = n^2 - n_a \tag{8}$$

Now, replacing Eq 8 in Eq 7, we have

$$AI = \frac{n_a + 1}{n^2 + 1 - n_a} \tag{9}$$

The value of n_a is $0 \leq n_a \leq n^2$, 0 when all pairs disagree and n^2 when all pairs agree.

$$\forall x \in n_a, \frac{1}{n^2 + 1} \leq AI(x) \leq n^2 + 1 \tag{10}$$

Hence, AI is a monotonically increasing function in the range of n_a.

enAMOSA follows the formulation of AMOSA [35]. The acceptance probability is crucial for the behavior of the simulated annealing. *enAMOSA* adopts a dynamic acceptance which is dependent on the domination status [35]. It is given by:

$$P_{acc} = \frac{1}{1 + \exp^{\frac{-\Delta E_{q,s,t}}{T}}} \tag{11}$$

where, $\Delta E_{q,s,\,t}$ represents the change in energy state of state q and state s at given temperature T. The convergence proof of simulated annealing based multi-objective optimization is elaborately explained in [41].

All the above mentioned factors ensure the convergence of the proposed algorithm.

Dataset collection and preparation

To evaluate the performance of the proposed algorithm we have used a total of 13 benchmark omic datasets. The details of the datasets are given in Table 1. The datasets are downloaded from the following repositories: The Cancer Genome Atlas (TCGA) https://tcga-data.nci.nih.gov/tcga/, NCBI GEO http://www.ncbi.nlm.nih.gov/geo and Memoral Sloan-Kettering Cancer Center (MSKCC)http://cbio.mskcc.org/cancergenomics/prostate/data/.

TCGA.BRC. This Breast cancer the dataset contains samples from patients with invasive tumors. It contains data for three views: miRNASeq(Level 3), RNAseq and DNA Methylation. Using PAM50 classifier [42, 43] patients were classified into four categories: Her2, Basal, LumA, LumB.

OXF.BRC.1. This Breast cancer [1][44] dataset contains data for three views: microRNA expression (GSE22220 accession number), mRNA (GSE22219 accession number) and DNA Methylation. Using PAM50 classifier [42, 43] patients were classified into four categories: Her2, Basal,LumA, LumB.

OXF.BRC.2. This Breast cancer [44] dataset contains data for three views: microRNA expression (GSE22220 accession number), mRNA (GSE22219 accession number) and DNA Methylation. Using clinical data also retrieved from the same source, patients were classified into four categories: Level1, Level2, Level3, Level4.

MSKCC.PRCA. This dataset contains samples from patients with prostate cancer tumors. It has three views: gene expression, miRNA expression and DNA Methylation. According to a study performed on this dataset [45], patients are grouped into two categories: first class is Tumor stage I and the second class is Tumor stage II, III and IV.

TCGA.GBM. Glioblastoma cancer the dataset has three views: gene expression, miRNA expression and DNA Methylation. As described in [46], patients are grouped into four categories: Classical, Mesenchymal, Neural and Proneural.

TCGA.OVG. Ovarian cancer dataset contain samples from patients with ovarian serous cystadenocarcinoma tumors. It has three views: gene expression, miRNA expression and DNA Methylation. Based on clinical stages, patients are grouped into four categories: class one: stage IA, IB, IC, IIA, IIB and IIC; class two: IIIA, IIIB and IIIC; class three: stage IV.

TCGA.COAD. Colon cancer dataset contain samples from patients suffering from Colon Adenocarcinoma (COAD). It has three views: gene expression, miRNA expression and DNA Methylation. Based on clinical stages, patients are grouped into four categories: class one: stage I, IA, IB, IC; class two: II, IIA, IIB and IIC; class three: III, IIIA, IIIB and IIIC; class four: stage IVA, IVB, IV.

TCGA.LIHC. Liver cancer dataset contain samples from patients with Liver Hepatocellular Carcinoma. It has three views: gene expression, miRNA expression and DNA Methylation. Based on clinical stages, patients are grouped into four categories: class one: stage I; class two: stage II; class three: IIIA, IIIB and IIIC; class four: stage IV.

Table 1. Descriptions of datasets.

Dataset	Views	Total Features	Selected Features	Samples
TCGA.BRC	RNASeq	20510	4300	621
	miRNASeq	1046	220	
	DNA Methylation	4885	1125	
OXF.BRC.1	Gene Expression	21439	4500	349
	miRNA Expression	734	164	
	DNA Methylation	4885	1125	
OXF.BRC.2	Gene Expression	21439	4500	349
	miRNA Expression	734	164	
	DNA Methylation	4885	1125	
MSKCC.PRA	Gene Expression	26446	5300	151
	miRNA Expression	368	82	
	DNA Methylation	3894	858	
TCGA.GBM	Gene Expression	12042	2500	274
	miRNA Expression	534	110	
	DNA Methylation	5000	1200	
TCGA.OVG	Gene Expression	12043	2500	398
	miRNA Expression	800	190	
	DNA Methylation	5000	1200	
TCGA.COAD	Gene Expression	20351	4883	220
	miRNA Expression	705	170	
	DNA Methylation	5000	1200	
TCGA.LIHC	Gene Expression	20531	4792	367
	miRNA Expression	705	170	
	DNA Methylation	5000	1200	
TCGA.LUSC	Gene Expression	20531	4880	341
	miRNA Expression	705	170	
	DNA Methylation	5000	1200	
TCGA.SKCM	Gene Expression	20531	4884	448
	miRNA Expression	705	170	
	DNA Methylation	5000	1200	
TCGA.SARC	Gene Expression	20531	4617	257
	miRNA Expression	1046	241	
	DNA Methylation	5000	1150	
TCGA.KIRC	Gene Expression	20531	4880	183
	miRNA Expression	705	170	
	DNA Methylation	5000	1200	
TCGA.AML	Gene Expression	20531	4520	170
	miRNA Expression	705	168	
	DNA Methylation	5000	1198	

https://doi.org/10.1371/journal.pone.0216904.t001

TCGA.LUSC. Lung cancer dataset contain samples from patients with Lung Squamous Cell Carcinoma. It has three views: gene expression, miRNA expression and DNA Methylation. Based on clinical stages, patients are grouped into four categories: class one: stage IA, IB, IC; class two: stage II, IIA, IIB; class three: stage III; and class four: stage IV.

TCGA.SKCM. Melanoma cancer dataset contain samples from patients with skin cutaneous melanoma (SKCM). It has three views: gene expression, miRNA expression and DNA

Methylation. Based on Clerk's level in clinical data, patients are grouped into four categories: class one: Level I; class two: Level II; class three: Level III; and class four: Level IV.

TCGA.SARC. The Cancer Genome Atlas Sarcoma (TCGA.SARC) contain samples from patients suffering from sarcoma. It has three views: gene expression, miRNA expression and DNA Methylation. Based on the sample types in clinical data, patients are grouped into four categories.

TCGA.KIRC. The Cancer Genome Atlas Kidney Renal Clear Cell Carcinoma (TCGA-KIRC) contain samples from patients suffering from kidney cancer. It has three views: gene expression, miRNA expression and DNA Methylation. Based on clinical stages, patients are grouped into four categories: class one: stage I; class two: stage II; class three: stage III; and class four: stage IV.

TCGA.AML. TCGA.AML dataset contain samples from patients suffering from Acute Myeloid Leukemia. It has three views: gene expression, miRNA expression and DNA Methylation. Based on clinical data, patients are divided into four categories.

Preprocessing of datasets

One of the common features of omics datasets is that the number of samples is much smaller than the number of features. Normalization of features in different omics is necessary for handling different distributions. Further, feature selection for dimensionality reduction is essential to provide different omics an equal prior opportunity to contribute to clustering. Dimensionality reduction is also crucial for keeping the most informative features, reducing the load on the clustering algorithm. In our approach, we have used an unsupervised feature selection technique, variance score. For this, we calculated the variance of each feature. Among them, top 22 − 24% features having highest scores are selected. The number of selected features for different benchmark datasets are given in Table 1.

Evaluation metrics

To compare enAMOSA with other methods we have used two evaluation metrics, *normalized mutual information* (NMI) [47] and *adjusted rand index* (ARI) [48]. These metrics measure the similarity between the true and predicted partitions; higher values signify predicted class is more similar to true class.

Results

Input parameters

The proposed approach, *enAMOSA*, is based on the multiobjective optimization technique, AMOSA [35]. It has three main components: (i) initial temperature value (T_{max}); (ii) cooling schedule; and (iii) number of iterations (*iter*) at each temperature.

The initial temperature is selected such that the algorithm can capture the entire search space. If initial temperature is set to too high, then it will accept all the proposed solutions and if set to too low it will transform into a greedy search. Here, the initial temperature (T_{max}) is set to achieve an initial acceptance rate of approximately 50% on derogatory proposals. Here, T_{min} is set to 10^{-3}. The initial temperature is selected based on the acceptance ratio of ζ, and average positive change in objective function, Δf_o [49].

$$T_{max} = -\frac{\Delta f_o}{\ln \zeta}$$

Table 2. Parameter settings for the proposed algorithm *enAMOSA*.

enAMOSA	
Max Temperature	100
Min Temperature	0.0001
# Iteration	100
Rate of cooling (α)	0.8
Soft Limit	40
Hard Limit	20

https://doi.org/10.1371/journal.pone.0216904.t002

Here $\zeta = 1/2$,

$$T_{max} = \frac{\Delta f_o}{\ln(2)}$$

The cooling schedule determines the functional form of the change in temperature required in SA [35]. The temperature is changed using commonly used geometric schedule, $T_{i+1} = \alpha \times T_i$, where α is the cooling rate and $0 < \alpha < 1$. As stated in [35], value of α is chosen between 0.5 to 0.99. This cooling schedule is simple in nature. There is a need for a small number of transitions to be sufficient to reach the thermal equilibrium. Here, the value of α is set to 0.8, causing a sufficiently small number of transitions in temperature to reach equilibrium.

The number of iterations at each temperature is chosen so that the system is sufficiently close to the stationary distribution at that temperature [35]. Less number of iterations will significantly reduce the search space, and the solution will not reach the global optimal. For our problem, as the sample size is not considerably large, the iteration value is set to 100.

In Table 2, we have reported the parameter settings used in the experiments.

Clustering performance

An extensive comparative study is performed to show the effectiveness of enAMOSA with respect to different approaches. The comparing approaches are briefly described below:

1. In order to show the effectiveness of using multiple clustering techniques to initialize the archive, we have developed different versions of enAMOSA clustering technique varying the base clustering algorithms. Abbreviations used *km*– K-means, *spec*– spectral, *cl*– complete linkage and *fs*– fast search. All these algorithms follow the exact steps of *enAMOSA*. Those are shown below:

   a. enAMOSA$_{km}$: this is the enAMOSA approach where only K-means clustering technique is used to generate the base partitionings. Here all the initial solutions of the archive are generated after running *K*-means clustering algorithm for different values of *K*. Other steps of this algorithm are very similar to those of *enAMOSA*.

   b. enAMOSA$_{cl}$: this is the enAMOSA approach where only complete linkage clustering technique is used to generate the base partitionings. Here all the initial solutions of the archive are generated after running complete linkage clustering technique for different values of *K*. Other steps of this algorithm are very similar to those of *enAMOSA*.

   c. enAMOSA$_{fs}$: this is the enAMOSA approach where only fast search clustering technique is used to generate the base partitionings. Here all the initial solutions of the archive are generated after running fast search clustering technique with different parameter values. Other steps of this algorithm are very similar to those of *enAMOSA*.

Table 3. Comparison of Normalized Mutual Information (NMI) scores of different combinations of our proposed approach.

	BRC	BRC.1	BRC.2	MSKCC	GBM	OVG	COAD	LIHC	LUSC	SKCM	SARC	KIRC	AML
enAMOSA$_{km,spec}$	0.4461	0.4714	0.3842	0.1495	0.4816	0.1194	0.1377	0.1209	0.3435	0.0814	0.09708	0.0910	0.4615
enAMOSA$_{km,cl}$	0.4131	0.4219	0.4692	0.0979	0.4401	0.1107	0.1201	0.0984	0.3321	0.0618	0.0483	0.0291	0.3078
enAMOSA$_{km,fs}$	0.4601	0.4679	0.4097	0.1401	0.4487	0.1303	0.1417	0.1334	0.3647	0.0796	0.1040	0.0951	0.5157
enAMOSA$_{cl,spec}$	0.4515	0.4653	0.3904	0.1425	0.4803	0.1147	0.1207	0.1134	0.3476	0.0784	0.0736	0.0891	0.4574
enAMOSA$_{cl,fs}$	0.4641	0.4730	0.4012	0.1498	0.4817	0.1203	0.1297	0.1219	0.3574	0.07807	0.1022	0.01074	0.5098
enAMOSA$_{spec,fs}$	0.4689	0.4717	0.4397	0.1521	0.4927	0.1104	0.1514	0.1298	0.3651	0.1126	0.1013	0.1095	0.5231
enAMOSA$_{km,cl,fs}$	0.4787	0.5105	0.4475	0.1735	0.5094	0.1394	0.1704	0.1473	0.3747	0.1319	0.0985	0.1025	0.5201
enAMOSA$_{cl,fs,spec}$	0.4702	0.5447	0.4778	0.1916	0.5407	0.2236	0.2012	0.1603	0.4096	0.1594	0.1102	0.1154	0.5487
enAMOSA$_{cl,spec,km}$	0.4707	0.4804	0.4584	0.1605	0.5146	0.1264	0.1537	0.13199	0.3815	0.1409	0.1017	0.0920	0.4701
enAMOSA$_{km,spec,fs}$	0.4772	0.5546	0.4760	0.2066	0.5419	0.2176	0.1952	0.1693	0.4106	0.1609	0.1130	0.1161	0.5507

https://doi.org/10.1371/journal.pone.0216904.t003

d. enAMOSA$_{spec}$: this is the enAMOSA approach where only spectral clustering technique is used to generate the base partitionings. Here all the initial solutions of the archive are generated after running spectral clustering technique with different values of K. Other steps of this algorithm are very similar to those of *enAMOSA*.

Further, as a part of our experimentation, we have also developed different versions of proposed *enAMOSA* approach where different combinations of size 2 / 3 base clustering algorithms are utilized for generating the initial solutions in the archive. Other steps of these approaches are very similar to those of *enAMOSA*. For Eg, *enAMOSA$_{km,spec}$*, uses the K-means and spectral clustering for generating base partitionings and follows the exact steps of *enAMOSA*. The results of these different variants of *enAMOSA* are shown in Tables 3 and 4.

2. In order to show the efficacy of ensemble based perturbation operator in enAMOSA process, we have developed another ensemble based multiobjective multi-view based approach, namely, AMOSA(ensemble). The steps of this approach are enumerated below:

    - The initialization of the archive will be done similar to that of enAMOSA. Four different clustering techniques, K-means, complete linkage, spectral and fast search clustering are executed multiple times with varying parameter values and the number of clusters. The membership matrices generated by these clustering techniques are encoded in the form of solutions of the archive.

Table 4. Comparison of Adjusted Rand Index (ARI) scores of different combinations of our proposed approach.

	BRC	BRC.1	BRC.2	MSKCC	GBM	OVG	COAD	LIHC	LUSC	SKCM	SARC	KIRC	AML
enAMOSA$_{km,spec}$	0.4007	0.3717	0.3212	0.0998	0.3921	0.1091	0.02851	0.0163	0.3164	0.03205	0.0987	0.1048	0.4015
enAMOSA$_{km,cl}$	0.3681	0.3402	0.2954	0.0481	0.3620	0.0493	0.0224	0.0098	0.1712	0.0216	0.0190	0.0401	0.3634
enAMOSA$_{km,fs}$	0.4116	0.3797	0.3207	0.1034	0.3975	0.1017	0.03196	0.0185	0.2705	0.0330	0.1045	0.1314	0.4184
enAMOSA$_{cl,spec}$	0.3918	0.3697	0.3102	0.0981	0.3816	0.1034	0.02961	0.0185	0.2624	0.03105	0.0991	0.1034	0.4087
enAMOSA$_{cl,fs}$	0.4066	0.3757	0.3198	0.1018	0.3943	0.1009	0.03114	0.0179	0.2695	0.0321	0.1051	0.1326	0.4161
enAMOSA$_{spec,fs}$	0.4216	0.4375	0.3792	0.1085	0.4369	0.1078	0.10184	0.0704	0.2459	0.0253	0.1098	0.1311	0.4201
enAMOSA$_{km,cl,fs}$	0.4291	0.5120	0.3915	0.1294	0.4593	0.1011	0.1211	0.0935	0.2901	0.0843	0.1057	0.1319	0.4198
enAMOSA$_{cl,fs,spec}$	0.4501	0.5284	0.4201	0.1513	0.4710	0.1012	0.1213	0.1016	0.3103	0.1023	0.1107	0.1402	0.4215
enAMOSA$_{cl,spec,km}$	0.4393	0.5101	0.40914	0.1302	0.4601	0.1008	0.1461	0.1015	0.3091	0.0879	0.1008	0.1084	0.4087
enAMOSA$_{km,spec,fs}$	0.4513	0.5304	0.4284	0.1601	0.4709	0.094	0.1437	0.1065	0.3002	0.0934	0.1103	0.1412	0.4208

https://doi.org/10.1371/journal.pone.0216904.t004

- For the perturbation operator we have used the following operator. The simple binary mutation is applied on each membership matrix encoded as a string with some probability. The binary bit value is flipped with some probability. Some points are randomly selected and their membership values are changed.
- In order to compute the objective functions, V number of membership matrices present in the string are obtained. The *conn-XB*-index values of all these V partitionings are calculated. The agreement index between these V partitionings is also calculated. The objective functions are $\left\{conn - XB_1, conn - XB_2, \ldots, conn - XB_V, \frac{1}{AI}\right\}$
- AMOSA process is applied to simultaneously minimize these objective functions.
  Note that the above process is different from the proposed approach only in the use of perturbation operator. Unlike enAMOSA here normal binary perturbation operations are used to generate new solutions. Thus initial solutions generated by base clustering algorithms were not ensembled during the optimization process. Each individual solution is evolved separately without mixing with other solutions. This algorithm is developed to show that ensemble based mutation operation indeed plays an important role in generating good solutions.

3. In order to show the potency of multiobjective based multiview clustering, we have also compared the performance of enAMOSA with state-of-the art multiview based classification techniques, namely MVDA (unsupervised) algorithm [16], LRAcluster [18], PINS [21], SNF [23] and iClusterBayes [28].

Using Eq 12, we have calculated the degree of contribution by each view in the final clustering obtained. Contributions computed for different views are shown in Fig 4.

$$Degree_v = \frac{\|Adj^v \cap Adj^{\cup v}\|}{\|Adj^{\cup v}\|} \qquad (12)$$

Here, Adj^v = the adjoint matrix of the partitioning obtained using view v $Adj^{\cup v}$ = the adjoint matrix corresponding to the final consensus partitioning.

Statistical significance test

For statistical significance test we have used a non-parametric test one-way Analysis of Variance (ANOVA) because it is independent of the distribution type of the dataset. The test is performed at 1% significance level. Results obtained by all the seven algorithms for each dataset are divided into seven groups. One-way ANOVA is conducted between enAMOSA group and remaining groups and results are reported in Table 5. All the p-values reported in Table 5 are less than 0.01. These values establish that improvements obtained by enAMOSA over other comparing algorithms are statistically significant.

Gene marker identification

From the clustering results obtained by enAMOSA on the OXF.BRC.1 dataset, we tried to extract the group of genes which have mainly contributed in patient classification. There are four patient classes in OXF.BRC.1 data set, viz., Her2, Basal, LumA, LumB. To identify the gene markers from Her2 class, we solved a binary classification problem. Two groups are created, one containing the samples from Her2 class and the other containing samples from rest of the classes. After considering both the groups, Signal-to-Noise Ratio (SNR) [50] is calculated

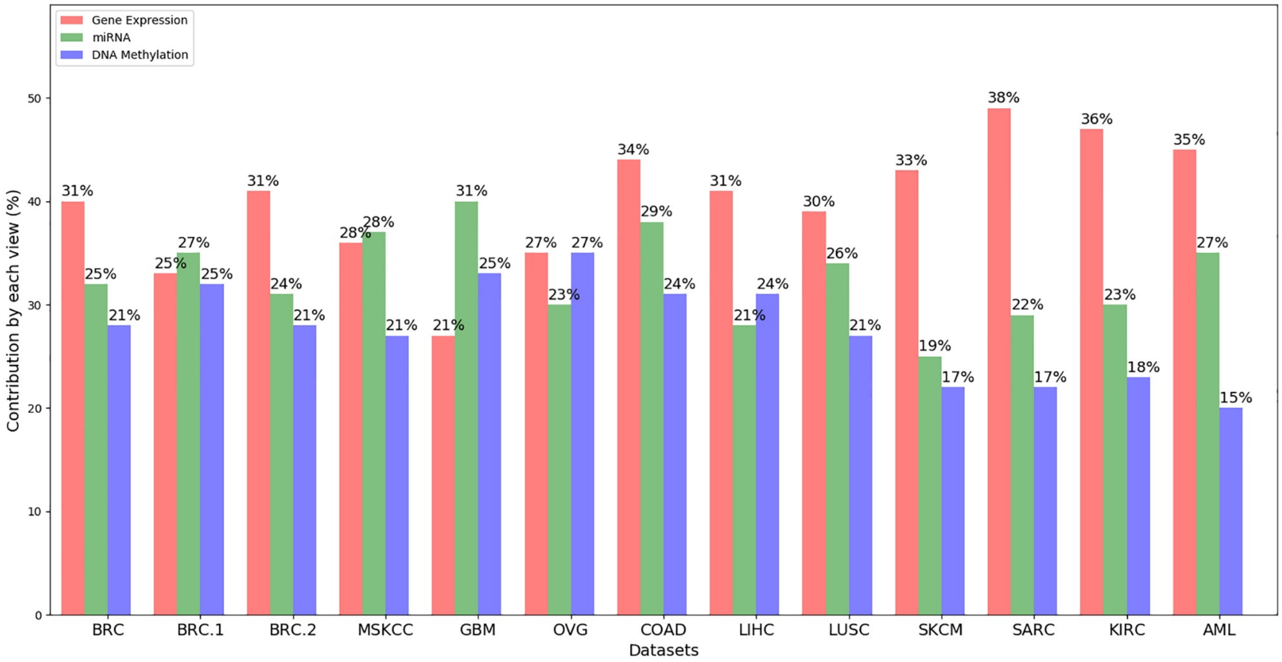

Fig 4. Contribution by each view in clustering.

https://doi.org/10.1371/journal.pone.0216904.g004

for each of the genes. It is defined as,

$$SNR = \frac{\mu_1 - \mu_2}{\sigma_1 + \sigma_2} \times 100, \tag{13}$$

where σ_j and μ_j, $j \in [1, 2]$, respectively, denote the standard deviation and the mean of class j for the corresponding gene. Higher SNR value for an individual gene signifies that it is having higher expression value for the class it belongs to and lower expression values for others. Finally total 10 genes are selected from the SNR list, with top 5 genes having highest SNR values (up regulated genes) and bottom 5 genes having lowest SNR values (down regulated genes). Similarly like Her2, the process is repeated for other classes too present in the dataset.

Gene markers for OXF.BRC.1 dataset. OXF.BRC.1 dataset is having 4 classes, so a total of 40 genes are obtained with 20 up regulated genes and 20 down regulated genes. Fig 5 shows

Table 5. The p-values reported by one-way ANOVA test on comparing *enAMOSA* with other methods.

	BRC	BRC.1	BRC.2	MSKCC	GBM	OVG	COAD	LIHC	LUSC	SKCM	SARC	KIRC	AML
enAMOSA$_{km}$	9.35e-36	1.38e-35	2.84e-44	8.46e-51	1.01e-31	1.61e-17	7.77e-4	5.65e-5	6.20e-10	9.05e-8	1.28e-5	3.56e-4	8.07e-5
enAMOSA$_{cl}$	3.94e-63	1.18e-54	7.69e-50	8.18e-65	3.28e-57	3.11e-22	5.32e-9	2.31e-7	3.67e-7	7.11e-10	2.01e-4	2.01e-7	3.17e-5
enAMOSA$_{spec}$	3.55e-15	3.08e-18	4.00e-20	1.93e-14	1.98e-28	1.79e-24	1.23e-8	2.14e-5	1.05e-11	8.12e-6	5.18e-5	2.28e-7	1.21e-4
enAMOSA$_{fs}$	1.28e-31	2.56e-30	7.07e-32	3.65e-41	6.22e-42	7.05e-25	3.24e-14	1.27e-9	5.42e-8	79.12e-7	6.65e-5	7.22e-4	6.05e-5
AMOSA (ensemble)	7.24e-25	5.05e-28	2.49e-31	1.78e-27	3.14e-33	2.82e-26	2.17e-24	3.24e-7	2.78e-8	5.31e-7	0.44e-7	5.12e-7	4.64e-6
LRAcluster	8.94e-28	3.11e-28	4.77e-26	7.84e-28	4.11e-28	2.57e-26	1.84e-13	3.76e-11	1.11e-4	1.61e-7	3.74e-8	4.41e-4	4.37e-5
PINS	1.44e-7	1.12e-7	8.64e-6	2.73e-7	8.93e-9	4.53e-5	2.44e-9	6.72e-6	6.50e-7	1.63e-4	3.08e-8	1.00e-4	1.93e-4
SNF	1.26e-12	5.71e-4	8.63e-8	7.64e-9	2.77e-5	6.23e-7	1.19e-7	6.34e-12	2.63e-10	6.22e-11	8.94e-9	7.53e-11	1.43e-9
iClusterBayes	0.0045	0.0118	0.0086	0	0.0357	0.0023	0.0076	0.0048	0.0034	0.0043	4.93e-9	4.51e-5	2.24e-10
MVDA	3.74e-12	1.41e-4	7.37e-7	1.24e-15	4.13e-6	8.73e-10	9.87e-11	1.45e-17	1.35e-5	7.86e-7	4.11e-8	2.57e-6	1.84e-3

https://doi.org/10.1371/journal.pone.0216904.t005

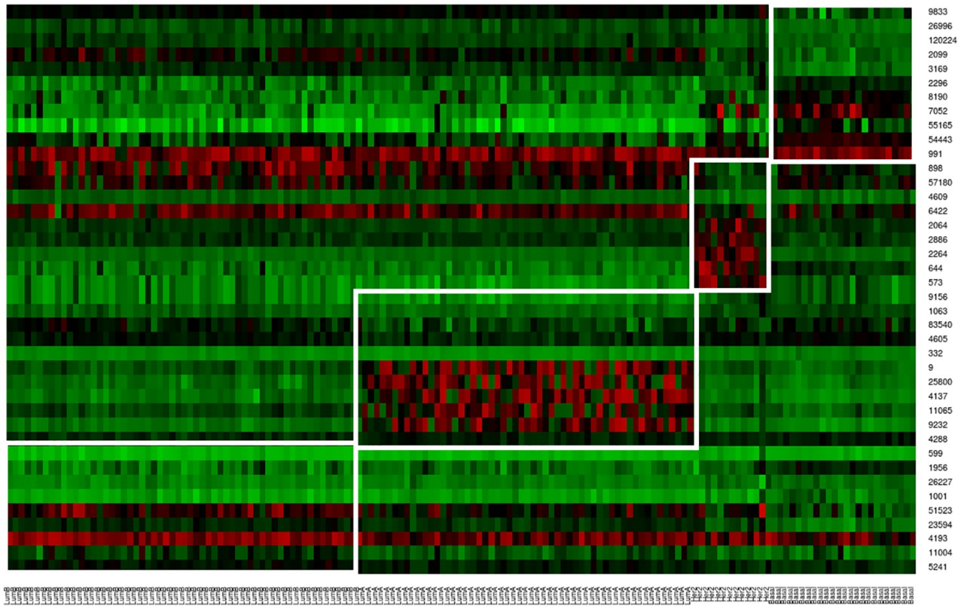

Fig 5. Heatmap to show the expression levels of the selected gene markers for each subclass in OXF.BRC.1 dataset.

https://doi.org/10.1371/journal.pone.0216904.g005

the heatmap plot of these genes along with their class names on X-axis. Here red signifies higher expression levels, green signifies lower expression levels and black signifies moderate expression levels. It is also seen from the Fig 5 that for a particular tumor class identified genes are either up-regulated or down-regulated. List of selected gene markers for Her2, Basal, LumA, LumB classes are reported in Table 6. Note that a gene up-regulated in one class can be down-regulated in another.

Biological significance test

To show the biological significance of selected genes, a biological significance test is conducted using Gene ontology consortium (http://www.geneontology.org/). For each GO term, the percentage of genes sharing that term among the genes of that cluster (% Cluster) and among the

Table 6. Selected 10 gene markers for OXF.BRC.1 dataset.

Her2		Basal		LumA		LumB	
Gene ID	Down/Up	Gene ID	Down/Up	Gene ID	Down/Up	Gene ID	Down/Up
2064	Down	2296	Down	9	Down	51523	Down
2886	Down	8190	Down	25800	Down	23594	Down
2264	Down	7052	Down	4137	Down	4193	Down
644	Down	55165	Down	11065	Down	11004	Down
573	Down	54443	Down	9232	Down	5241	Down
991	Up	9833	Up	9156	Up	4288	Up
898	Up	26996	Up	1063	Up	599	Up
57180	Up	120224	Up	83540	Up	1956	Up
4609	Up	2099	Up	4605	Up	26227	Up
6422	Up	3169	Up	332	Up	1001	Up

https://doi.org/10.1371/journal.pone.0216904.t006

Table 7. Significant shared Gene Ontology (GO) terms by gene markers.

Classes	Gene Ontology(GO) term	(%) Genome	(%)Cluster
Her2	regulation of catalytic activity: GO:0050790	47%	50%
	regulation of cell proliferation: GO:0042127	31%	40%
	negative regulation of programmed cell death: GO:0043069	50%	50%
	negative regulation of apoptotic process: GO:0043066	2%	20%
	positive regulation of cell proliferation: GO:0008284	3%	40%
	negative regulation of cell death: GO:0060548	5%	38%
Basal	biological process: GO:0008150	50%	50%
	biological regulation: GO:0065007	52%	60%
	signal transduction: GO:0007165	6%	10%
	nitrogen compound metabolic process: GO:0006807	27%	30%
	multicellular organismal process: GO:0032501	3%	30%
LumA	cell cycle: GO:0007049	30%	46%
	regulation of chromosome organization: GO:0033044	2%	20%
	organelle fission: GO:0048285	3%	10%
	regulation of chromosome segregation: GO:0051983	8%	10%
	mitotic nuclear division: GO:0140014	3%	20%
LumB	regulation of biological process: GO:0050789	17%	20%
	regulation of cellular process: GO:0050794	0.5%	10%
	multicellular organism development: GO:0007275 GO:0007275	1.3%	10%
	regulation of macromolecule metabolic process: GO:0060255	16%	20%
	organic substance biosynthetic process: GO:1901576	21%	30%

https://doi.org/10.1371/journal.pone.0216904.t007

whole genome (%Genome) has been reported in Table 7. From the results, it can be seen that the genes belonging to the same cluster share a higher percentage of GO terms compared to the whole genome. This signifies that the genes of a particular cluster are more involved in the similar biological process compared to the remaining genes of the genome.

Discussion

The average NMI and ARI values obtained by the execution (20 times) of our proposed method, enAMOSA, on all the 13 datasets are shown in Tables 8 and 9, respectively. From the Tables 8 and 9, it is observed that the results obtained by our proposed methodology outperform the results obtained by other state-of-the-art single objective algorithms (MVDA (unsupervised) algorithm [16], LRAcluster [18], PINS [21], SNF [23] and iClusterBayes [28]) by 10 − 11% (approx.) and 10 − 14% (approx.) in terms of NMI and ARI, respectively. Comparison of *enAMOSA* with other baseline versions (enAMOSA$_{km}$, enAMOSA$_{spec}$, enAMOSA$_{cl}$ and enAMOSA$_{fs}$) shows that combination of all the four base partitions (i.e., *enAMOSA*) performs better than its single base partition counterparts (enAMOSA$_{km}$, enAMOSA$_{spec}$, enAMOSA$_{cl}$ and enAMOSA$_{fs}$) by 5 − 10% (approx.) and 8 − 11%(approx.) in terms of NMI and ARI, respectively. To show the effectiveness of the new perturbation operator, *enAMOSA* is compared with *AMOSA(ensemble)*. NMI and ARI scores obtained by *enAMOSA* exceed *AMOSA(ensemble)* by 5 − 9%(approx.) and 8 − 10% (approx.), respectively. Results reflect the efficiency of the proposed integrated approach of ensemble and multi-objective algorithm through new perturbation operator over using them separately.

To further explore the importance of diversity in the base partitions, all possible combinations of the base partitions are generated and the results of NMI and ARI are presented in

Table 8. Comparison of Normalized Mutual Information (NMI) scores of our proposed approach (*enAMOSA*) with other baseline approaches and state-of-the art methods.

	BRC	BRC.1	BRC.2	MSKCC	GBM	OVG	COAD	LIHC	LUSC	SKCM	SARC	KIRC	AML
enAMOSA	**0.5092**	**0.5714**	**0.4980**	**0.2296**	**0.5649**	**0.2347**	**0.2151**	**0.1894**	**0.4216**	**0.1809**	**0.1147**	**0.1208**	**0.5607**
enAMOSA$_{km}$	0.4021	0.4185	0.3618	0.0906	0.4383	0.0797	0.0971	0.0594	0.3021	0.0281	0.0463	0.0184	0.3017
enAMOSA$_{cl}$	0.4067	0.4206	0.3531	0.1076	0.4354	0.0814	0.1014	0.0498	0.2841	0.0212	0.0315	0.0281	0.2962
enAMOSA$_{spec}$	0.4215	0.4418	0.3615	0.1206	0.4519	0.1067	0.1098	0.0961	0.3196	0.0684	0.0748	0.0907	0.4517
enAMOSA$_{fs}$	0.4375	0.4668	0.3798	0.1179	0.4708	0.1201	0.1147	0.0948	0.3089	0.0716	0.1005	0.1104	0.5141
AMOSA (ensemble)	0.4581	0.5071	0.4104	0.1390	0.4615	0.1421	0.1227	0.1103	0.3284	0.1097	0.1091	0.1109	0.5207
LRAcluster	0.0146	0.0232	0.0118	0.1098	0.0532	0.0304	0.0328	0.0573	0.0672	0.0483	0.0475	0.0389	0.3629
PINS	0.0118	0.0146	0.00392	0.0572	0.0153	0.0095	0.0459	0.0348	0.0237	0.0382	0.0262	0.0279	0.2219
SNF	0.0358	0.0475	0.0153	0.0098	0.0026	0.0068	0.0332	0.0129	0.0082	0.0088	0.0233	0.0908	0.4349
iClusterBayes	0.0121	0.09931	0.0153	0.0780	0.0306	0.0081	0.0106	0.0258	0.0112	0.0044	0.0177	0.0108	0.0894
MVDA	0.3912	0.4034	0.3403	0.1124	0.4213	0.0863	0.0793	0.0175	0.2594	0.0195	0.0321	0.0655	0.2871

https://doi.org/10.1371/journal.pone.0216904.t008

Tables 3 and 4 respectively. Comparing these results with that obtained by the proposed algorithm *enAMOSA* (from Tables 8 and 9) it is observed that the proposed method outperforms its counterparts by 2 – 4% (approx.) for both NMI and ARI. The following observations are drawn from careful analysis of the results in Tables 3 and 4:

1. The hypothesis of the work is that the diversity in the initial solutions will allow the algorithm to capture more accurate cluster structures. From Tables 3 and 4, we can see that the NMI and ARI values obtained by combined base partitions are higher compared to their single counterparts in Tables 8 and 9 respectively. Further, within Tables 3 and 4 it is seen that combination of 3 base partitions produces higher results compared to the combination of 2 base partitions. For example, results obtained by $enAMOSA_{cl,km,spec}$ are better compared to any of its 2 base partitions like $enAMOSA_{cl,km}$, $enAMOSA_{cl,spec}$ and $enAMOSA_{km,spec}$. Similar results are true for other combinations also that are reported in Tables 3 and 4. Results support the initial hypothesis of the work.

2. The performance of the algorithm depends on the type of base partitions used for populating the archive initially. In the worst case scenario, *enAMOSA* generates results comparable to the best base partition solution the archive is initialized with. By this we mean that, suppose initially the archive is initialized with solutions obtained from two different base

Table 9. Comparison of Adjusted Rand Index (ARI) scores of our proposed approach (*enAMOSA*) with other baseline methods and state-of-the art methods.

	BRC	BRC.1	BRC.2	MSKCC	GBM	OVG	COAD	LIHC	LUSC	SKCM	SARC	KIRC	AML
enAMOSA	**0.4723**	**0.5534**	**0.4414**	**0.1721**	**0.4809**	**0.1157**	**0.1461**	**0.1215**	**0.3471**	**0.1105**	**0.1215**	**0.1537**	**0.4315**
enAMOSA$_{km}$	0.3641	0.3471	0.2815	0.0448	0.3561	0.0430	0.02051	0.0083	0.1573	0.0161	0.0189	0.0384	0.3412
enAMOSA$_{cl}$	0.3651	0.3384	0.2901	0.0457	0.3620	0.0473	0.02110	0.0082	0.1615	0.0186	0.0175	0.0115	0.3603
enAMOSA$_{spec}$	0.3805	0.3547	0.2981	0.0935	0.3726	0.0984	0.02751	0.0096	0.2136	0.0228	0.0984	0.1045	0.3942
enAMOSA$_{fs}$	0.3916	0.3675	0.3102	0.0958	0.3864	0.0953	0.02814	0.0094	0.2219	0.0231	0.1041	0.1308	0.4107
AMOSA (ensemble)	0.3943	0.3861	0.3306	0.1006	0.3937	0.1002	0.0447	0.0108	00.2419	0.0259	0.1114	0.1137	0.4208
LRAcluster	0.0086	0.0112	0.0012	0.0105	0.0076	0.0051	0.0184	0.0054	0.0098	0.0055	0.0263	0.0392	0.2546
PINS	0.0144	0.0112	0.00864	0.01142	0.0089	0.0045	0.0244	0.0067	0.0065	0.0016	0.0152	0.0136	0.1195
SNF	0.0126	0.0057	0.0863	0.00081	0.0027	0.0062	0.0119	0.0063	0.0026	0.00062	0.0238	0.0157	0.3667
iClusterBayes	0.0045	0.0118	0.0086	0.0171	0.0357	0.0023	0.0076	0.0048	0.0034	0.0043	0.0399	0.0288	0.0482
MVDA	0.2457	0.3441	0.2831	0.067	0.3441	0.0614	0.0194	0.0085	0.1351	0.0145	0.02366	0.0355	0.2021

https://doi.org/10.1371/journal.pone.0216904.t009

Table 10. F1-measure and accuracy values obtained by *enAMOSA* for all the datasets.

Datasets	F1-measure	Accuracy
TCGA.BRC	0.6592	0.6814
OXF.BRC.1	0.7048	0.7184
OXF.BRC.2	0.6067	0.6126
MSKCC	0.5146	0.5541
TCGA.GBM	0.6975	0.7068
TCGA.OVG	0.5012	0.5236
TCGA.COAD	0.4905	0.5131
TCGA.LIHC	0.4718	0.4946
TCGA.LUSC	0.6056	0.6479
TCGA.SKCM	0.4861	0.4931
TCGA.SARC	0.4315	0.4415
TCGA.KIRC	0.4174	0.4212
TCGA.AML	0.6904	0.6882

https://doi.org/10.1371/journal.pone.0216904.t010

algorithms, one producing good results and other producing bad. Final results obtained from *enAMOSA* will be comparable to that of the good results. For example, for dataset *SARC* in Table 8, we can see *enAMOSA*$_{km}$ and *enAMOSA*$_{fs}$ provide NMI values of 0.0184 and 0.1005, respectively. When the partitions obtained from base algorithms Kmeans and fast search are used jointly, the NMI result obtained by *enAMOSA*$_{km,fs}$ on *SARC* dataset is 0.1040, reported in Table 3. By analyzing Tables 3 and 4, it is observed that similar pattern is followed for other datasets also. At least, *enAMOSA* ensures to generate best possible solution among the base partitions.

3. From Tables 3 and 4, it is also observed that enAMOSA$_{km,spec,fs}$ performs better than other algorithms presented in these tables for most of the datasets. A closer analysis shows that mainly density-based clustering algorithms (fast search and spectral clustering) capture better structures from the datasets compared to K-means and hierarchical. It may be because density-based clustering algorithms are capable of capturing arbitrary cluster structures from the datasets.

Apart from NMI and ARI scores, we have also reported the F1-measure and accuracy score obtained by *enAMOSA* on all the 13 benchmark datasets in the Table 10.

In Fig 6, we have reported the gene expression profile plot for each individual classes (Basal, Her2, LumA and LumB) of OXF.BRC.1 dataset. The compactness of the structures shows that

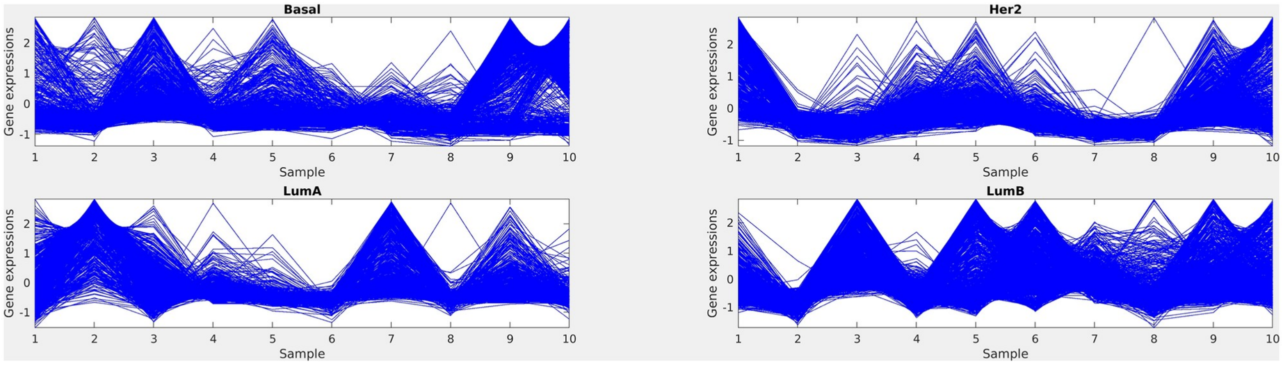

Fig 6. Gene expression profile plot for each subclass in OXF.BRC.1 dataset.

https://doi.org/10.1371/journal.pone.0216904.g006

Table 11. Execution time of the algorithms in seconds.

	BRC	BRC.1	BRC.2	MSKCC	GBM	OVG	COAD	LIHC	LUSC	SKCM	SARC	KIRC	AML
enAMOSA	9531.21	4389.12	4380.98	727.08	2045.80	4419.02	2241.11	4373.24	4352.51	6533.02	3016.14	2045.03	978.42
LRAcluster	15034.51	3421.16	3415.77	972.30	2055.93	3417.27	2104.53	5918.45	5074.86	8550.49	3057.00	1569.91	1025.22
PINS	1219.78	612.71	614.45	121.45	356.52	634.88	379.28	371.29	596.02	798.99	376.72	379.28	206.98
SNF	65.71	19.61	20.71	12.04	13.72	20.07	15.89	27.21	24.31	36.23	17.30	15.89	14.90
iClusterBayes	9041.95	4503.10	4523.06	1014.06	2923.39	4543.08	3635.03	5669.00	5309.83	6776.40	4197.39	3635.03	1847.40
MVDA	222.11	146.73	140.27	153.54	190.24	136.37	197.62	224.15	141.09	214.08	175.583	211.07	225.11

https://doi.org/10.1371/journal.pone.0216904.t011

the clustered samples share the same type of gene expressions, i.e, within a cluster genes have good coherence among them.

In Table 11, we have reported the execution time (in seconds) for all the algorithms used in the experiment. All the algorithms are executed on machine having intel Core i5 7th Generation processor with 8GB of RAM. The time is calculated by taking the average over 20 runs of the algorithms. Execution time of *enAMOSA* is comparable to that of *LRAcluster* and *iClusterBayes*.

Scalability analysis

An important aspect of performance analysis is the study of how algorithm performance varies with parameters. In particular, we may evaluate the scalability of the algorithm, that is, how effectively it can use an increased number of samples. From the time complexity equation, Eq 6, it is observed that the execution time of the model depends on the total number of iterations (*TotalIter*), number of samples (n), number of clusters (r), size of archive (N) and number of objective functions (M). Now, the total number of iteration (*TotalIter*), size of archive (N) and number of objective functions (M) are fixed for all the datasets. As for the number of clusters are concerned, in our algorithm, the number of clusters is not fixed for any particular dataset, the algorithm automatically determines the number of clusters. So, the increase in execution time depends on the number of samples (n) present in the datasets. By analyzing the numeric values obtained by empirical studies in Table 11, clearly supports our finding. *TCGA. BRC* has the highest number of samples (629), it has the highest execution time of 9631.21 seconds and *MSKCC.PRA* has the lowest number of samples (151), it has the lowest execution time of 727.08 seconds. Similar kind of results are seen for other datasets also in Table 11, that is, execution time increases with an increase in sample points. The results reported in Table 11 reveals that the execution time of the algorithm is not huge with the increase in the number of samples in the data set; it converges in polynomial time even with a large number of samples and also the execution time is comparable to the state-of-the-art method *iClusterBayes*.

Conclusion

In order to properly subclassify the patient data, consideration of multiple views is highly solicited. A single clustering method is not enough to capture all possible structures in a dataset. This is a multi-view classification problem which is solved with the help of the proposed multi-objective based multi-view cluster ensemble based technique.

In the current paper, we have proposed a multiobjective based cluster ensemble technique for multi-view classification. Initially different simple clustering algorithms are applied to generate some base partitionings by varying the number of clusters. These initial solutions are finally combined using some cluster ensemble based operators. The goodness of the individual partitionings obtained using different views is measured using a connectivity-based internal cluster validity index, namely *conn-XB* and an agreement index computing the agreement amongst the partitionings captured on different views. The values of these measures are simultaneously optimized using the search capability of AMOSA, which is a multiobjective simulated annealing based optimization technique. Obtained results on 13 cancer data sets illustrate the utility of the proposed approach for patient sub-classification task. An extensive comparative study has been conducted to show the efficacy of individual components of the proposed enAMOSA approach. Some approaches are developed to show the utility of initialization step of enAMOSA; further another multi-view based cluster ensemble technique is developed which utilizes some normal mutation operators instead of using an ensemble-based operator. This comparative study reveals that all the components of the proposed approach, enAMOSA are important.

Some of the important findings we made are (i) proposed algorithm successfully captures complex heterogeneous structures from multi-omics data compared to other state-of-the-art methodology; (ii) the proposed perturbation operator proves effective in integrating the ensemble technique with multi-objective technique. The comparative results support its effectiveness; (iii) the algorithm, *enAMOSA*, effectively combines multiple views having different number of clusters; (iv) the execution time of the algorithm is not huge; it converges in polynomial time and also the execution time is comparable to the state-of-the-art method *iCluster-Bayes*. Study of the various comparative results presented in this paper supports our findings.

In future research, works will be carried out in developing a multi-view based biclustering framework. The developed multi-view based clustering techniques will be applied for solving some real-life problems of social media data. Documents can also be represented using multiple views. Thus many of the document classification problems can be solved using the developed multiobjective based multi-view clustering technique.

Author Contributions

Conceptualization: Sayantan Mitra, Sriparna Saha.

Formal analysis: Sayantan Mitra.

Investigation: Sayantan Mitra.

Methodology: Sayantan Mitra.

Supervision: Sriparna Saha.

Validation: Sayantan Mitra.

Visualization: Sayantan Mitra.

Writing – original draft: Sayantan Mitra.

Writing – review & editing: Sayantan Mitra, Sriparna Saha.

References

1. Khan J, Wei JS, Ringner M, Saal LH, Ladanyi M, Westermann F, et al. Classification and diagnostic prediction of cancers using gene expression profiling and artificial neural networks. Nature medicine. 2001; 7(6):673–679. https://doi.org/10.1038/89044 PMID: 11385503
2. Chang HY, Nuyten DS, Sneddon JB, Hastie T, Tibshirani R, Sørlie T, et al. Robustness, scalability, and integration of a wound-response gene expression signature in predicting breast cancer survival. Proceedings of the National Academy of Sciences of the United States of America. 2005; 102(10): 3738–3743. https://doi.org/10.1073/pnas.0409462102 PMID: 15701700
3. Huang E, Cheng SH, Dressman H, Pittman J, Tsou MH, Horng CF, et al. Gene expression predictors of breast cancer outcomes. The Lancet. 2003; 361(9369):1590–1596. https://doi.org/10.1016/S0140-6736(03)13308-9

4. Vang Nielsen K, Ejlertsen B, Møller S, Trøst Jørgensen J, Knoop A, Knudsen H, et al. The value of TOP2A gene copy number variation as a biomarker in breast cancer: Update of DBCG trial 89D. Acta oncologica. 2008; 47(4):725–734. https://doi.org/10.1080/02841860801995396

5. Faceli K, de Carvalho AC, de Souto MC. Cluster ensemble and multi-objective clustering methods. In: Pattern Recognition Technologies and Applications: Recent Advances. IGI Global; 2008. p. 325–343.

6. Faceli K, de Souto MC, de Araújo DS, de Carvalho AC. Multi-objective clustering ensemble for gene expression data analysis. Neurocomputing. 2009; 72(13-15):2763–2774. https://doi.org/10.1016/j.neucom.2008.09.025

7. Li Y, Wang J, Zhao D, Li G, Chen C. A two-stage approach for combined heat and power economic emission dispatch: Combining multi-objective optimization with integrated decision making. Energy. 2018; 162:237—254. https://doi.org/10.1016/j.energy.2018.07.200.

8. Saha S, Bandyopadhyay S. Some connectivity based cluster validity indices. Applied Soft Computing. 2012; 12(5):1555–1565. https://doi.org/10.1016/j.asoc.2011.12.013

9. Saha S, Mitra S, Kramer S. Exploring Multiobjective Optimization for Multiview Clustering. ACM Trans Knowl Discov Data. 2018; 20(2):44:1–44:30. https://doi.org/10.1145/3182181

10. An L, Doerge R. Dynamic clustering of gene expression. ISRN Bioinformatics. 2012; 2012. https://doi.org/10.5402/2012/537217 PMID: 25969750

11. Wang Y, Pan Y. Semi-supervised consensus clustering for gene expression data analysis. BioData mining. 2014; 7(1):7. https://doi.org/10.1186/1756-0381-7-7 PMID: 24920961

12. Saha S, Kaushik K, Alok AK, Acharya S. Multi-objective semi-supervised clustering of tissue samples for cancer diagnosis. Soft Computing. 2016; 20(9):3381–3392. https://doi.org/10.1007/s00500-015-1783-5

13. de Souto MC, Costa IG, de Araujo DS, Ludermir TB, Schliep A. Clustering cancer gene expression data: a comparative study. BMC bioinformatics. 2008; 9(1):497. https://doi.org/10.1186/1471-2105-9-497 PMID: 19038021

14. Saha S, Ekbal A, Gupta K, Bandyopadhyay S. Gene expression data clustering using a multiobjective symmetry based clustering technique. Computers in biology and medicine. 2013; 43(11):1965–1977. https://doi.org/10.1016/j.compbiomed.2013.07.021 PMID: 24209942

15. Paul S, Maji P. City block distance for identification of co-expressed MicroRNAs. In: International Conference on Swarm, Evolutionary, and Memetic Computing. Springer; 2013. p. 387–396.

16. Serra A, Fratello M, Fortino V, Raiconi G, Tagliaferri R, Greco D. MVDA: a multi-view genomic data integration methodology. BMC bioinformatics. 2015; 16(1):261. https://doi.org/10.1186/s12859-015-0680-3 PMID: 26283178

17. Sun S. A survey of multi-view machine learning. Neural Computing and Applications. 2013; 23(7-8): 2031–2038. https://doi.org/10.1007/s00521-013-1362-6

18. Wu D, Wang D, Zhang MQ, Gu J. Fast dimension reduction and integrative clustering of multi-omics data using low-rank approximation: application to cancer molecular classification. BMC genomics. 2015; 16(1):1022. https://doi.org/10.1186/s12864-015-2223-8 PMID: 26626453

19. Wang X, Qian B, Ye J, Davidson I. Multi-objective multi-view spectral clustering via pareto optimization. In: Proceedings of the 2013 SIAM International Conference on Data Mining. SIAM; 2013. p. 234–242.

20. Hoadley KA, Yau C, Wolf DM, Cherniack AD, Tamborero D, Ng S, et al. Multiplatform analysis of 12 cancer types reveals molecular classification within and across tissues of origin. Cell. 2014; 158(4): 929–944. https://doi.org/10.1016/j.cell.2014.06.049 PMID: 25109877

21. Nguyen T, Tagett R, Diaz D, Draghici S. A novel approach for data integration and disease subtyping. Genome research. 2017; p. gr–215129. https://doi.org/10.1101/gr.215129.116

22. Chikhi NF. Multi-view clustering via spectral partitioning and local refinement. Information Processing & Management. 2016; 52(4):618–627.

23. Wang B, Mezlini AM, Demir F, Fiume M, Tu Z, Brudno M, et al. Similarity network fusion for aggregating data types on a genomic scale. Nature methods. 2014; 11(3):333. https://doi.org/10.1038/nmeth.2810 PMID: 24464287

24. Speicher NK, Pfeifer N. Integrating different data types by regularized unsupervised multiple kernel learning with application to cancer subtype discovery. Bioinformatics. 2015; 31(12):i268–i275. https://doi.org/10.1093/bioinformatics/btv244 PMID: 26072491

25. Zhang X, Zong L, Liu X, Yu H. Constrained NMF-Based Multi-View Clustering on Unmapped Data. In: AAAI; 2015. p. 3174–3180.

26. Shen R, Olshen AB, Ladanyi M. Integrative clustering of multiple genomic data types using a joint latent variable model with application to breast and lung cancer subtype analysis. Bioinformatics. 2009; 25(22):2906–2912. https://doi.org/10.1093/bioinformatics/btp543 PMID: 19759197

27. Mo Q, Wang S, Seshan VE, Olshen AB, Schultz N, Sander C, et al. Pattern discovery and cancer gene identification in integrated cancer genomic data. Proceedings of the National Academy of Sciences. 2013; p. 201208949.

28. Mo Q, Shen R, Guo C, Vannucci M, Chan K, Hilsenbeck S. A fully Bayesian latent variable model for integrative clustering analysis of multi-type omics data. Biostatistics (Oxford, England). 2018; 19(1): 71–86. https://doi.org/10.1093/biostatistics/kxx017

29. Nie F, Tian L, Li X. Multiview clustering via adaptively weighted procrustes. In: Proceedings of the 24th ACM SIGKDD International Conference on Knowledge Discovery & Data Mining. ACM; 2018. p. 2022–2030.

30. Nie F, Li J, Li X. Self-weighted multiview clustering with multiple graphs. In: Proceedings of the Twenty-Sixth International Joint Conference on Artificial Intelligence; 2017. p. 2564–2570.

31. Faceli K, De Carvalho AC, De Souto MC. Multi-objective clustering ensemble. International Journal of Hybrid Intelligent Systems. 2007; 4(3):145–156. https://doi.org/10.3233/HIS-2007-4302

32. Strehl A, Ghosh J. Cluster ensembles—a knowledge reuse framework for combining multiple partitions. Journal of machine learning research. 2002; 3(Dec):583–617.

33. Fern XZ, Brodley CE. Solving cluster ensemble problems by bipartite graph partitioning. In: Proceedings of the twenty-first international conference on Machine learning. ACM; 2004. p. 36.

34. Rappoport N, Shamir R. Multi-omic and multi-view clustering algorithms: review and cancer benchmark. Nucleic Acids Research. 2018; 46(20):10546–10562. https://doi.org/10.1093/nar/gky889 PMID: 30295871

35. Bandyopadhyay S, Saha S, Maulik U, Deb K. A simulated annealing-based multiobjective optimization algorithm: AMOSA. IEEE transactions on evolutionary computation. 2008; 12(3):269–283. https://doi.org/10.1109/TEVC.2007.900837

36. Jain AK, Murty MN, Flynn PJ. Data clustering: a review. ACM computing surveys (CSUR). 1999; 31(3): 264–323. https://doi.org/10.1145/331499.331504

37. Rodriguez A, Laio A. Clustering by fast search and find of density peaks. Science. 2014; 344(6191): 1492–1496. https://doi.org/10.1126/science.1242072 PMID: 24970081

38. Karypis G, Kumar V. METIS–unstructured graph partitioning and sparse matrix ordering system, version 2.0. 1995;.

39. Xie XL, Beni G. A validity measure for fuzzy clustering. IEEE Transactions on pattern analysis and machine intelligence. 1991; 13(8):841–847. https://doi.org/10.1109/34.85677

40. Shapira O, Wachs J. A Graphical method based on the Xie-Beni Validity index to improve the 'Possibilistic C-Means with Repulsion'Algorithm. In: Proc. of the 4th Intl. Symp on Intelligent Manufact. Systems; 2004. p. 958–967.

41. Villalobos-Arias M, Coello CAC, Hernández-Lerma O. Asymptotic convergence of a simulated annealing algorithm for multiobjective optimization problems. Mathematical Methods of Operations Research. 2006; 64(2):353–362. https://doi.org/10.1007/s00186-006-0082-4

42. Tibshirani R, Hastie T, Narasimhan B, Chu G. Diagnosis of multiple cancer types by shrunken centroids of gene expression. Proceedings of the National Academy of Sciences. 2002; 99(10):6567–6572. https://doi.org/10.1073/pnas.082099299

43. Parker JS, Mullins M, Cheang MC, Leung S, Voduc D, Vickery T, et al. Supervised risk predictor of breast cancer based on intrinsic subtypes. Journal of clinical oncology. 2009; 27(8):1160–1167. https://doi.org/10.1200/JCO.2008.18.1370 PMID: 19204204

44. Buffa FM, Camps C, Winchester L, Snell CE, Gee HE, Sheldon H, et al. microRNA associated progression pathways and potential therapeutic targets identified by integrated mRNA and microRNA expression profiling in breast cancer. Cancer research. 2011; p. canres–0489. https://doi.org/10.1158/0008-5472.CAN-11-0489 PMID: 21737487

45. Ray B, Henaff M, Ma S, Efstathiadis E, Peskin ER, Picone M, et al. Information content and analysis methods for multi-modal high-throughput biomedical data. Scientific reports. 2014; 4:4411. https://doi.org/10.1038/srep04411 PMID: 24651673

46. Verhaak RG, Hoadley KA, Purdom E, Wang V, Qi Y, Wilkerson MD, et al. Integrated genomic analysis identifies clinically relevant subtypes of glioblastoma characterized by abnormalities in PDGFRA, IDH1, EGFR, and NF1. Cancer cell. 2010; 17(1):98–110. https://doi.org/10.1016/j.ccr.2009.12.020 PMID: 20129251

47. Studholme C. Measures of 3D medical image alignment. University of London; 1997.

48. Hubert L, Arabie P. Comparing partitions. Journal of classification. 1985; 2(1):193–218. https://doi.org/10.1007/BF01908075

49. Suman B, Kumar P. A survey of simulated annealing as a tool for single and multiobjective optimization. Journal of the operational research society. 2006; 57(10):1143–1160. https://doi.org/10.1057/palgrave.jors.2602068

50. Golub TR, Slonim DK, Tamayo P, Huard C, Gaasenbeek M, Mesirov JP, et al. Molecular classification of cancer: class discovery and class prediction by gene expression monitoring. science. 1999; 286(5439):531–537. https://doi.org/10.1126/science.286.5439.531 PMID: 10521349